



ELSEVIER

Available online at www.sciencedirect.com

SCIENCE @ DIRECT®

Journal of Sound and Vibration 290 (2006) 337–368

JOURNAL OF
SOUND AND
VIBRATION

www.elsevier.com/locate/jsvi

Multistage gearbox condition monitoring using motor current signature analysis and Kolmogorov–Smirnov test

Chinmaya Kar, A.R. Mohanty*

Mechanical Engineering Department, Indian Institute of Technology, Kharagpur, 721302, India

Received 1 March 2004; received in revised form 22 February 2005; accepted 2 April 2005

Available online 1 September 2005

Abstract

Even though there are a number of condition monitoring and analysis techniques, researchers are in search of a simple and easy way to monitor vibration of a gearbox, which is an omnipresent and an important power transmission component in any machinery. Motor current signature analysis (MCSA) has been the most recent addition as a non-intrusive and easy to measure condition monitoring technique.

The objective of this paper is to detect artificially introduced defects in gears of a multistage automotive transmission gearbox at different gear operations using MCSA as a condition monitoring technique and Kolmogorov–Smirnov (KS) test as an analysis technique assuming that any defect or load has a specific probability distribution. Empirical cumulative distribution functions (ECDF) are used to differentiate these probability distributions. Steady as well as fluctuating load conditions on the gearbox are tested for both vibration and current signatures during different gear operations. It is concluded that combined MCSA and KS test can be an effective way to monitor and detect faults in gears.

© 2005 Elsevier Ltd. All rights reserved.

1. Introduction

Condition monitoring of a gearbox is a vital activity because of its importance in power transmission in any industry. Therefore, there has always been a constant endeavor to improve upon the monitoring techniques and analysis tools for the early detection of faults in the gearbox.

*Corresponding author. Tel.: +91 3222 282944; fax: +91 3222 255303.

E-mail address: amohanty@mech.iitkgp.ernet.in (A.R. Mohanty).

Nomenclature	
A_{sT} & A_{sM}	amplitudes due to torque producing and magnetizing current components
d_i	i th defective case
D -stat (k)	statistic used in the K S test
D_{critical}	critical value of D -stat
D^+ & D^-	one-tailed D -stat
F_i	ECDF of the i th data set ($i = 1, 2$)
f_e	the supply line frequency (50 Hz)
f_{ecc}	frequency of the sidebands of f_e due to rotor eccentricities
f_{brb}	frequencies of the sidebands of f_e due to broken rotor bar
f_{bng}	frequencies of the sidebands of f_e due to bearing frequencies
f_{load}	sidebands of f_e due to frequency of the load
f_r	rotating shaft frequency
$G(x)$	exact null distribution
H	handle to the decision of null hypothesis
I_s	stator current in any phase
N	total number of data
N_1 & N_2	number of data points,
p	number of poles in the induction motor.
p -value	probability value
s	slip in the induction motor
X_i	the random variable at i th position
α	significance level
β_1	correction factor
ϕ	phase angle

Techniques such as wear and debris analysis, vibration monitoring and acoustic emissions require accessibility to the gearbox either to collect samples or to mount the transducers on or near the gearbox. But dusty environment, background noise, structural vibration etc. may hamper the quality and efficiency of these techniques. Hence, there is a need to monitor the gearbox away from its actual location, which can be achieved through motor current signature analysis (MCSA), which has already been successfully applied to condition monitoring of induction motor and in bearings [1,2]. But its application to gear condition monitoring is a new area which has been investigated recently by Mohanty and Kar [3,4].

Signal processing techniques such as Cepstrum analysis [5], Wigner–Ville distribution [6], wavelet transform [3,7]; and some statistical techniques such as beta distribution [8], correlation dimension [9], Kolmogorov–Smirnov (KS) test [10,11], have found application in gear fault diagnosis through vibration and acoustics monitoring of gearbox. KS test has already been used in ball bearing fault diagnosis by Kar and Mohanty [12] and in differentiating rotor-stator rub by Hall and Mba [13]. But its application to MCSA has been first given in Refs. [3,4] for analyzing current transients due to load fluctuation.

In Refs. [10,11], Andrede et al. have used KS probability distribution in distinguishing the difference amongst brand new gear, normal operating gear, worn-out gear and gears with artificially introduced fatigue cracks. But these papers considered a single stage spur gear and did not take account of the change in load conditions. Moreover, they had found the technique effective in distinguishing the cracks when taking the largest fatigue crack as reference signal. Kar and Mohanty [12] were successful in implementing KS test in ball bearing fault diagnosis. A number of artificially introduced faults in inner race, outer race and balls could be distinguished when compared with good bearings using the D -stat; the statistic of KS test; and its probability value (p -value). Hall and Mba [13] introduced KS test to acoustic emission due to shaft-seal rubbing. They used one-sample KS test with Rayleigh, Gaussian, etc. distribution as the known distribution.

The types of artificial defects introduced in gears have been classified by Staszewski et al. [14] as root crack, wear and tear, and tooth breakage. In Ref. [15], these authors have described various time-varying parameters that act as sources of excitation in helical gears. These parameters are gear mesh stiffness and damping, friction force and torque, bearing force, static transmission error (due to profile and deflection) and backlash. It has been found that with a tooth breakage in helical gear, a transient appear in one rotation of the gear/pinion in the gear mesh stiffness, damping, and friction force and torque. Choy and Mugler [16] have inferred that wear and tear; which is uniform for all teeth; causes a shift in phase in the gear mesh stiffness. Similarly, root crack of the tooth affects the deflection part of the static transmission error [7]. These authors [3] have studied cases of breakage of one tooth and two teeth removed in a helical gear, which has two or three teeth in contact at any time, and also three gears are under synchro-meshed condition implying 6–9 number of lines of contact at any meshing conditions. Moreover, maximum operating load was 5.625 kW, which is much lower than rated load of 35 kW of the gearbox.

In this paper, condition monitoring of a multistage gearbox is recommended using MCSA as the condition monitoring technique and two-sample KS test and empirical cumulative distribution function (ECDF) as the analysis techniques. The alternate hypothesis assumed here is that any change in defect or load condition of the gearbox will change the probability distributions of the amplitudes of the current and vibration signatures, and hence can be monitored. A multistage automotive transmission gearbox test-setup as shown in Fig. 1 is chosen for experimentation. Artificially introduced defective gears have been fitted in the gearbox and analysis was done at 2nd and 3rd gear operations. Fluctuating load conditions have also been studied in order to test the effect of load. Table 1 illustrates the types of defects, and steady and fluctuating loads applied to the gearbox. KS test is also applied to vibration signatures in order to compare and highlight the effectiveness of MCSA.

2. Theory

2.1. Motor current signature analysis

The current in a defect-free 3- ϕ induction motor at steady load operation will have an ideal sinusoidal waveform with a 50 Hz supply line frequency in all its phases such as R-phase, Y-phase and B-phase except at the time of starting when there will be transients in the current signatures. Some authors [17,18] have studied these stator current transients at the starting time for condition monitoring of induction motors. But later, steady stator currents are investigated to detect faults in induction motors such as rotor eccentricities, broken rotor bar and rolling element bearing damage, the review of which has been described in Refs. [1,2]. These defects produce sidebands across the supply line frequency given by following equations:

$$f_{\text{ecc}} = f_e \left[1 \pm m \left(\frac{1-s}{p/2} \right) \right] \quad \text{where } m = 1, 2, 3, \dots, \quad (1)$$

$$f_{\text{brb}} = f_e \left[k \left(\frac{1-s}{p/2} \right) \pm s \right] \quad \text{where } k/(p/2) = 1, 5, 7, \dots, \quad (2)$$

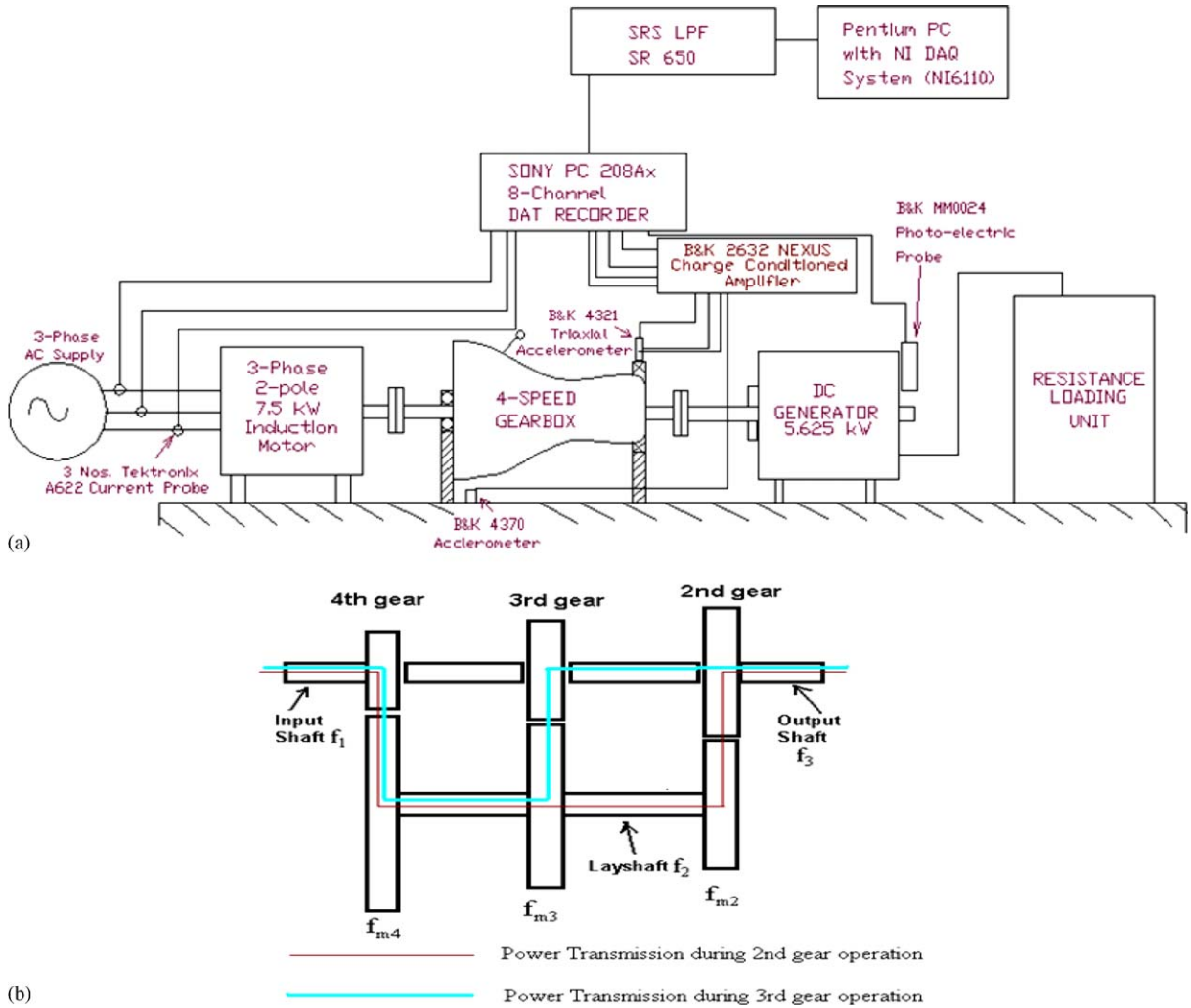


Fig. 1. (a) The schematic diagram of the experimental setup with instrumentation details, (b) The line diagram of the gearbox showing path of power transmission during 2nd and 3rd gear operation.

Table 1
Types of artificial defects introduced in gears

Sl. no.	Helical gear	Type of defect	Steady loads (kW)	Load transients (kW)
1	—	No defect ($d0$)	0	1.875
2	Second gear (main)	One tooth broken ($d1$)	0.75	3.75
3	Second gear (main)	Two teeth broken ($d2$)	1.875	5.625
4	Second gear (lay shaft)	Two teeth broken ($d3$)	3.0	
5	Third gear (main)	One tooth broken ($d4$)	3.75	
6	Third gear (main)	Two teeth broken ($d5$)	5.625	

$$f_{\text{bng}} = |f_e \pm mf_v| \text{ where } m = 1, 2, 3, \dots \tag{3}$$

The bearing characteristics frequencies include inner-race defect frequency, outer-race defect frequency and ball defect frequency.

It has also been observed in Ref. [19] that the sidebands due to oscillating torque and rotor eccentricity are difficult to be separated:

$$f_{\text{load}} = f_{\text{ecc}} = f_e \left[1 \pm m \left(\frac{1-s}{p/2} \right) \right] \text{ where } m = 1, 2, 3, \dots \tag{4}$$

Yacamini et al. [20] have suggested that any component having torsional vibration with a specific frequency will be reflected in the motor current as the sidebands across supply line frequency f_e as given in Eq. (5). This theory has been confirmed in Refs. [3,4] for a number of defect frequencies, where the motor current signatures for driving an automotive transmission gearbox have been studied. It has been found that the vibration signature has three rotating shaft frequencies and three gear mesh frequencies (GMF), and the sidebands of these frequencies are reflected in the current signature of any phase:

$$I_s = I_0 \cos(2\pi f_e t) + \left(\frac{A_{sT} + A_{sM}}{2} \right) \cos(2\pi(f_e - f)t - \phi) + \left(\frac{A_{sT} - A_{sM}}{2} \right) \cos(2\pi(f_e + f)t + \phi). \tag{5}$$

2.2. Kolmogorov–Smirnov test

The authors [12] have explained the fundamentals of KS test in details. In this paper, reviews of the equations used in KS test are covered. KS test is a non-parametric test assuming a null and alternate hypothesis as follows:

Null hypothesis ($H_0(H = 0)$): Two data sets have same probability distributions.
 Alternate hypothesis ($H_1(H = 1)$): Two data sets have different probability distributions.

Here, H is used as a handle to the decision. The statistic used for the decision is called D -stat, which is the maximum difference between the ECDF of the two data sets (F_1 and F_2) given by Eq. (6). The ECDF can be found using Eq. (7):

$$D - \text{stat} = \text{Sup}_X |F_1(X_i) - F_2(X_i)| \quad \forall i = 1, 2, \dots, N, \tag{6}$$

$$\begin{aligned} (X_i) &= P(X_i \leq x) = i/N \quad (\text{higher estimate probability}) \\ &= (i - 1)/N \quad (\text{lower estimate probability}), \end{aligned} \tag{7}$$

Where N is the total number of data and X_i is the random variable at i th position when the random variables are arranged in ascending order, and supremum means maximum. Zhang et al. [21] used an extended KS statistic to determine the number of components in a mixture model that can be used as statistical classification of data sets. Ferryanto [22] has applied two-dimensional KS test to two spectral distribution functions of two structures in order to detect structural changes of textures. Conover [23] has classified the two-sample KS test as one-sided KS test or

both sided KS test by Eqs. (6) and (8a,b), respectively. He has also provided formulae for exact two-sided p -value given by Eq. (9). The exact null distribution is shown in Eq. (10) for two-sided KS test. The detail descriptions of one-sample KS test have not been shown in this paper:

$$D^+ = \text{Sup}_X [F_1(X_i) - F_2(X_i)] \tag{8(a)}$$

and

$$D^- = \text{Sup}_X [F_2(X_i) - F_1(X_i)], \tag{8(b)}$$

$$p\text{-value} = 2 \frac{\binom{2N}{N+ND}}{\binom{2N}{N}} \text{ for equal data sizes } N. \tag{9}$$

$$G(X) = \left[1 - \frac{\binom{2N}{N} + c}{\binom{2N}{N}} \right]^2 \text{ where } c \text{ is the greatest integer less than } XN. \tag{10}$$

Greenwell and Finch [24] have given the asymptotic p -value for the D -stat for N_1 and N_2 tends to infinity:

$$p\text{-value} = Q\left(D\sqrt{\frac{N_1N_2}{N_1+N_2}}\right), \tag{11}$$

where

$$Q(z) = 2 \sum_{k=1}^{\infty} (-1)^{k-1} e^{-2k^2z^2}. \tag{12}$$

Since the actual value of N_1 and N_2 are finite, hence a correction factor β_1 shown in Eq. (13) is used. The corrected p -value is given by Eq. (14):

$$\beta_1 = \begin{cases} \frac{0.32N_1}{N_2^{1.5}} & \text{for } N_1 \text{ a multiple of } N_2, \\ \frac{0.25}{\sqrt{N_1}} & \text{otherwise,} \end{cases} \tag{13}$$

$$p\text{-value} = Q\left(D\sqrt{\frac{N_1N_2}{N_1+N_2}} + \beta_1\right). \tag{14}$$

Andrede et al. [9,10] have used a similar probability distribution as in Eq. (12) where the value of z is shown in Eq. (15):

$$z = \left(\sqrt{\frac{N_1N_2}{N_1+N_2}} + 0.12 + \frac{0.11}{\sqrt{(N_1N_2)/(N_1+N_2)}} \right) D. \tag{15}$$

Some other application can be found in Refs. [25,26]. Kozmann et al. [25] used K–S distance maps to classify different body surface potential maps (BSPM) citing an example of application of KS test in Bio-medical engineering; whereas Albano and Rapp [26] applied KS test to correlation integral in order to distinguish two system dynamics whose correlation dimensions are same.

In this paper, the D -stat and ECDF has been found using Eqs. (6) and (7). The p -value has been taken only to take decision regarding the acceptance or rejection of the null hypothesis and found out by the combination of Eqs. (12) and (15), same as the probability distribution taken by Andered et al. [9,10], but unlike these references, this paper will consider the D -stat as the main parameter and for the decision, the following rule will be applied:

$$H = \begin{cases} 0 & \text{if } D < D_{\text{critical}} \text{ or } p\text{-value} > \alpha, \\ 1 & \text{otherwise,} \end{cases} \quad (16)$$

where α = significance level generally taken as 0.05 and critical value of D -stat [27] can be found approximately from Eq. (17):

$$D_{\text{critical}} = 1.36 \sqrt{\frac{N_1 + N_2}{N_1 N_2}}. \quad (17)$$

Example of finding the value of D -stat and the effect of noise, DC component and time lagging has been shown in Appendix A.

3. Experimental setup

3.1. Gearbox test rig

The experimental setup consists of a 7.5 kW induction motor drawing power through a control panel and driving a 4-stage automotive transmission gearbox, a separately-excited DC generator of 5.625 kW capacity that is coupled to the output shaft of the gearbox and connected to a resistance loading unit to apply or remove load into the gearbox. The schematic diagram of the setup with instrumentation details is shown in Fig. 1a. For recording vibration and current signatures, the details of the instrumentation is explained in Ref. [3].

The 4-stage transmission gear has 2nd, 3rd, and 4th gear as synchro-mesh; and hence, at any operation of 2nd, 3rd, and 4th gear, three rotating shaft frequencies such as input shaft frequency, lay shaft frequency, and output shaft frequency; and three GMF such as 2nd GMF, 3rd GMF and 4th GMF will be active in the system. Fig. 1b shows the line diagram of gearbox with path of the power transmission during 2nd and 3rd gear operations.

Defects are introduced in the 2nd main gear and 2nd lay shaft gear as shown in Figs. 2(a)–(c). Similarly, in the 3rd main gear, two types of defects are introduced. Table 1 gives the type of defects introduced artificially to different gears. When one tooth and two teeth are removed from the 2nd gear, the defects will be known as $d1$ and $d2$ conditions, respectively. A two-teeth broken 2nd lay shaft gear will be termed as $d3$; and one or two teeth broken 3rd gear will be known as $d4$ and $d5$. When there is no defect in gear, it will be termed as $d0$ condition. The teeth were removed by die-sinking electro-discharge machining (EDM).

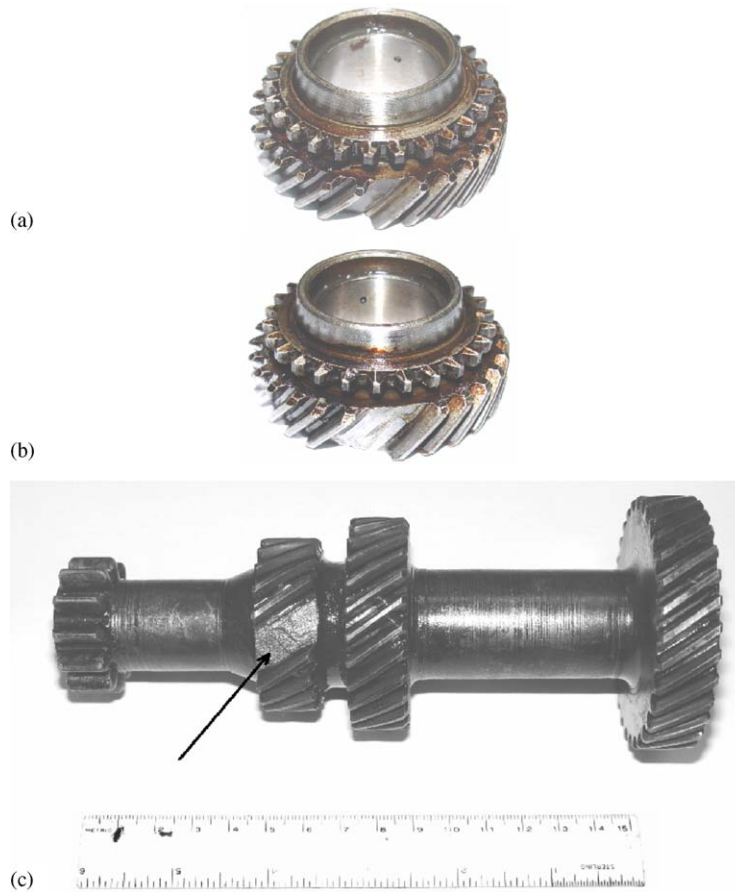


Fig. 2. Artificial defects introduced in different gears: (a) $d1$, (b) $d2$, (c) $d3$.

3.2. Analysis and data acquisition process

The analysis procedure is mainly categorized into steady signal analysis and transient signal analysis. For steady signal analysis, both current and vibration signals are acquired for 2nd and 3rd gear operations at four different steady load conditions such as 5.625, 3.75, 1.875 and 0 kW. In total, 8192 numbers of data were acquired with a sampling frequency of 4.096 kHz, for a total time length of 2 s duration. For steady load condition, the analysis bandwidth was from 0–2 kHz.

To analyze the effect of load fluctuation, transient analysis is done by sudden removal of load, and 8192 numbers of data were acquired with a sampling frequency of 20.48 kHz. The analysis bandwidth was 0–10 kHz. Three cases of such load fluctuations are considered in this paper, which are as follows:

Case-I:	1.875–0 kW
Case-II:	3.75–0 kW
Case-III:	5.625–0 kW

4. Results and discussions

After examining all the signals, only the lateral (horizontal) vibration signatures of the accelerometer, and current signatures of the R-phase have been chosen for analysis. First, vibration signatures with all defect and steady load conditions at 2nd gear operations are tested with two-sample KS test and then this step is repeated with current signatures, and for the vibration and current signatures under steady load condition for 3rd gear operation. Similarly, for transient analysis, KS test is applied to vibration and current transients due to load fluctuations for both 2nd and 3rd gear operations. In this paper, for the signature analysis, the combined defective and steady load conditions are expressed with simplified terms; for example, no defect and 5.625 kW load conditions is termed as $d0: 5.625$. For transient analysis of signatures, $d0:III$ will be substituted for no defect conditions with Case III i.e. 5.625 kW load fluctuation. The parameters of the KS tests are D -stat (k), p -value (p) and handle (H).

4.1. Operation with steady loads

4.1.1. Vibration signatures under steady loads: 2nd gear operation

The vibration signatures at 5.625 kW steady load and various defect conditions for the 2nd gear operations are shown in Figs. 3(a)–(f). It can be observed that with introduction of defects, the maximum amplitude as well as the amplitude distribution vary with type of defects which can be measured by several statistical parameters such as kurtosis, rms, etc. But in Ref. [12], it has been proved that except D -stat, all other statistical parameters yield inconsistent result, which cannot be used for detection purpose. Hence, D -stat and ECDF are used to measure the amplitude distribution, for which signals at all load and defective conditions are tested among themselves and the parameters of KS test such as D -stats (k), p -values (p) and handle (h) are tabulated as shown in Table 2, which is symmetric. The ECDFs for these signals at 5.625 kW load conditions are shown in Fig. 4a. To highlight the effect of load fluctuation at a particular defect, Fig. 4b is drawn for $d1$ condition at four steady loads. Fig. 4c shows D -stats when all the signatures are compared with that at no load and no defect conditions ($d0:0$). Two more steady load conditions such as 0.75 and 3 kW are added in the figure to confirm the trend. The following observations are noted from the tables and these figures:

1. 2nd gear defects such as $d1$, $d2$ and $d3$ can easily be detected at all load conditions during 2nd gear operation, the difference is much prominent at higher load conditions; whereas 3rd gear defects such as $d4$ and $d3$ are difficult to be traced at high load (Fig. 4c). Even, 1 defect in 3rd gear ($d4$) is having a similar probability distribution of amplitudes when compared with no defect conditions.
2. When vibration signature with no load is compared with that with 5.625 kW load for no defect condition, the resulting D -stat is 0.0398 whereas when it is compared with $d1: 0$ kW condition, the value of D -stat of 0.0317, giving an illusion that $d0: 5.625$ is having higher ECDF than $d1: 0$, but when these are compared with themselves, the D -stat is 0.0623. This is the reason why all the conditions have to be compared among themselves in order to reach a conclusion. But in case of $d3:0$ condition, the ECDF of $d0: 5.625$ case is having higher ECDF, which signifies the contention of this paper to consider load condition while detecting defects in gears.

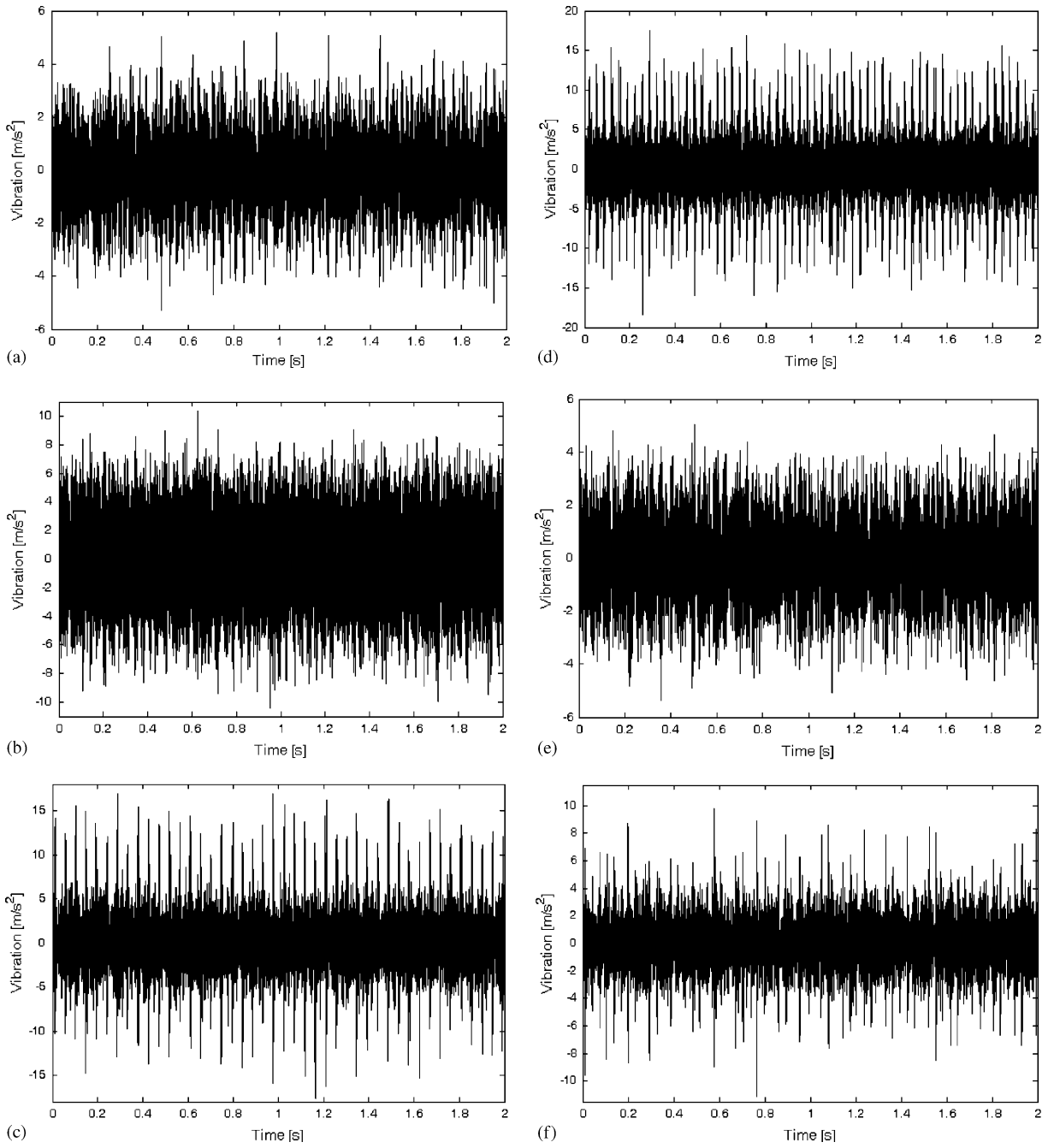


Fig. 3. The time-domain vibration signatures of gears at 5.625 kW steady load for various defective conditions during 2nd gear operation: (a) d_0 , (b) d_1 , (c) d_2 , (d) d_3 , (e) d_4 , and (f) d_5 .

Table 2 (continued)

	d0:0	d0:1.875	d0:3.75	d0:5.625	d1:0	d1:1.875	d1:3.75	d1:5.625	d2:0	d2:1.875	d2:3.75	d2:5.625	d3:0	d3:1.875	d3:3.75	d3:5.625	d4:0	d4:1.875	d4:3.75	d4:5.625	d5:0	d5:1.875	d5:3.75	d5:5.625	
d4:1.875	H																								
	P																								
	k																								
d4:3.75	H																								
	P																								
	k																								
d4:5.625	H																								
	P																								
	k																								
d5:0	H																								
	P																								
	k																								
d5:1.875	H																								
	P																								
	k																								
d5:3.75	H																								
	P																								
	k																								
d5:5.625	H																								
	P																								
	k																								

d0:3.75: no defect at 3.75 kW steady load, H: handle to the decision, p: p-value, k: D-stat.

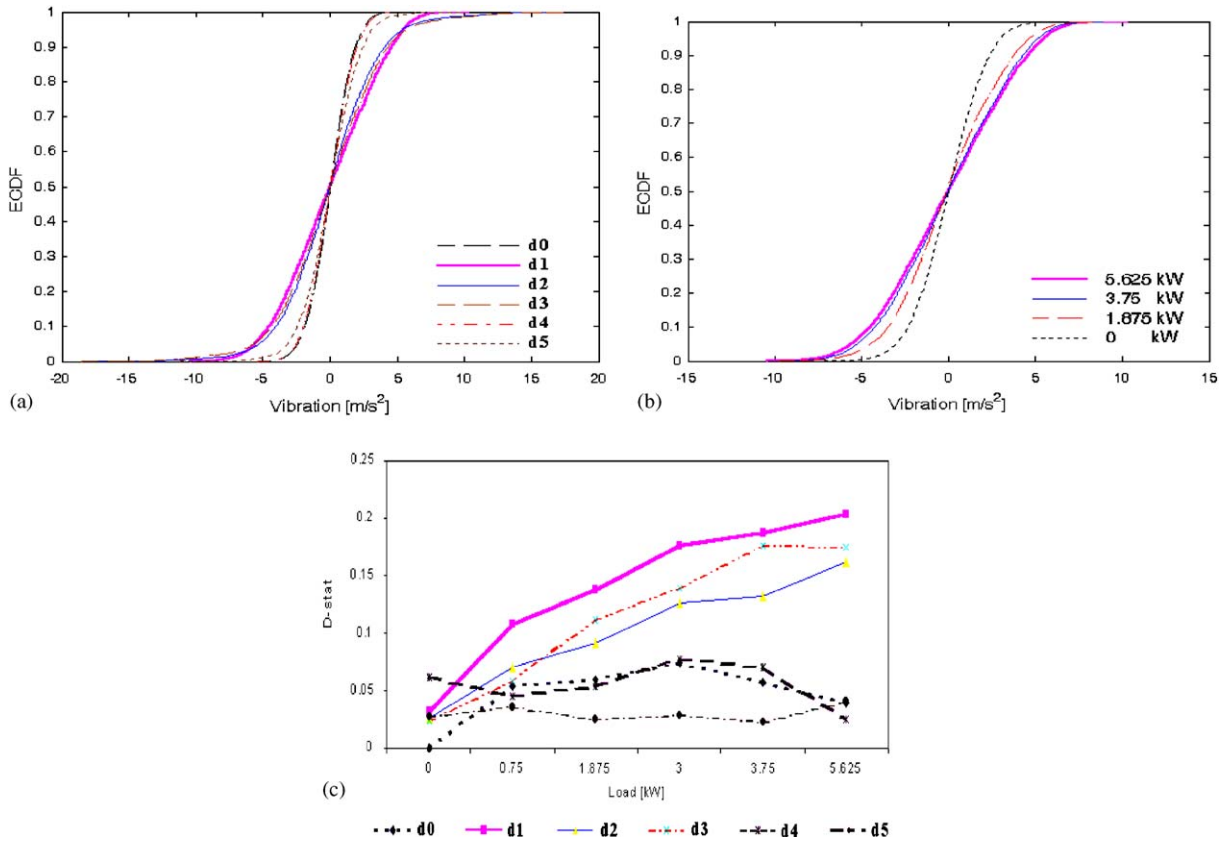


Fig. 4. Summary of Table 2: (a) ECDF of vibration signatures of all defective conditions at 5.625 kW steady load, (b) ECDF of all steady load conditions for *d1* condition, (c) *D*-stat variation with load considering vibration signature for no load and no defect condition as basis.

3. For a particular defect (*d1*), decrease in steady load decreases the ECDF below the intersection point as shown in Fig. 4b.
4. Though the *d1* condition is having lower maximum amplitude of vibration, it has much higher ECDF (shown in Fig. 4a) than those in *d2* and *d3* conditions. The following relation has been observed.

$$\text{Maximum amplitude of vibration : } d3 > d2 > d1$$

$$\text{Maximum ECDF : } d1 > d3 > d2.$$

This has been conformed by drawing the contour diagrams of discrete wavelet technique (shown in Figs. 5(a)–(d)) of the vibration signatures of all cases of 2nd gear defects and 5.625 kW load, by decomposing the signatures to 6 levels. In all the contour diagrams, it can be observed that the higher frequency region i.e. levels 1 and 2 are the energy carrier in gearbox vibration as these levels include the GMF and their harmonics. The energy possessed by a no defect condition (Fig. 5a) is very less, where as for defective conditions, the energy possessed by the signals are very high, because of the presence of impact. The *d1* condition (Fig. 5b) is

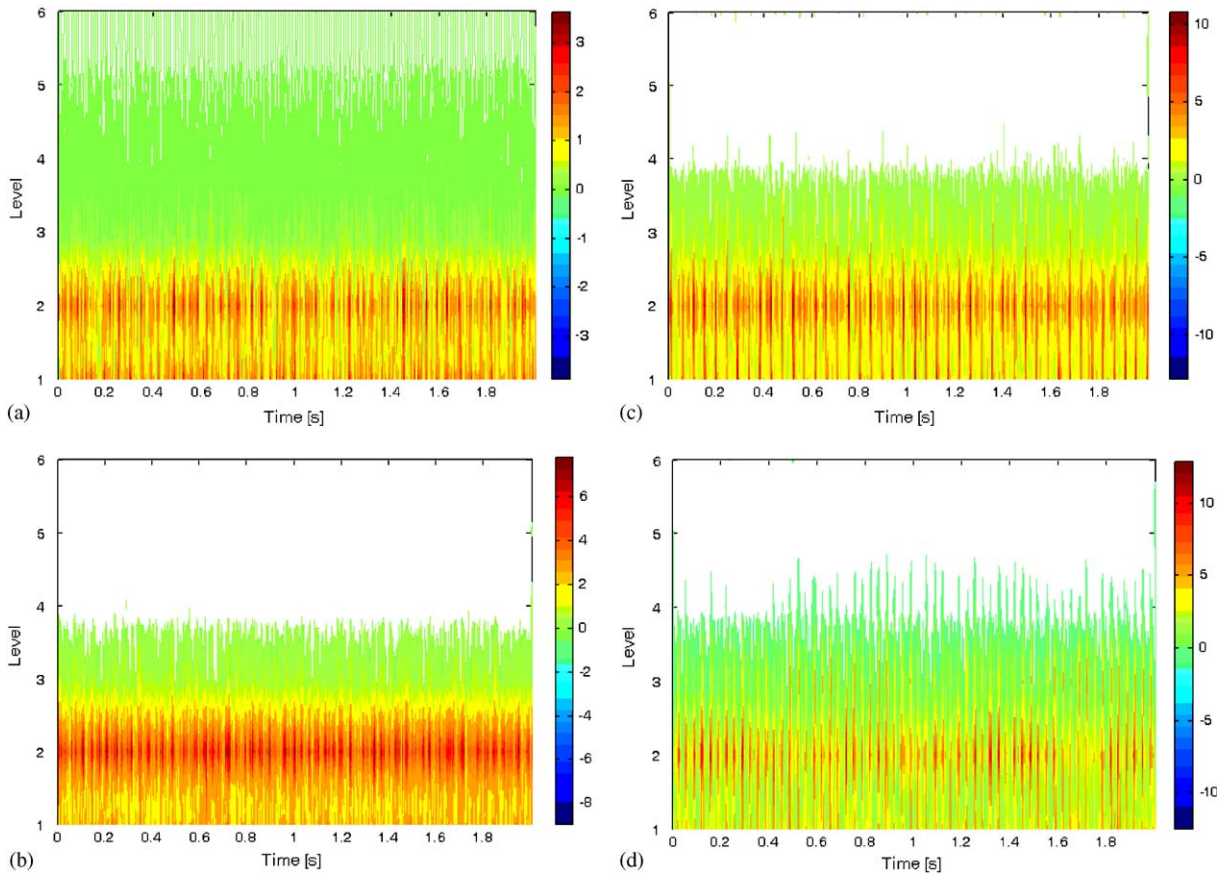


Fig. 5. DWT coefficients of vibration signatures for different defects in 2nd gear during 2nd gear operations at 5.625 kW steady load conditions: (a) d_0 , (b) d_1 , (c) d_2 and (d) d_3 .

characterized with less impact, hence lower maximum amplitude of vibration; and a gradual decrease in amplitudes causing a higher ECDF. The d_3 condition is characterized by large impact, with energy dispersed to levels 1–3, and hence a medium ECDF.

4.1.2. Motor current signatures under steady loads: 2nd gear operation

The time-domain signature of current with no defect and 5.625 kW steady load condition is mainly sinusoidal in nature due to the dominant 50 Hz line frequency and feeble sidebands of rotating and gear-mesh frequencies [3,4]. Question arises whether KS test will be able to differentiate the current signals for defect-free and defective gears or not. After applying KS test to various conditions, Table 3 is formed that shows the D -stats and the corresponding p -values when the current signatures at four steady loads and all defective cases are compared among themselves. Since, the table is symmetric, only the upper triangular part has been shown. The ECDFs of current signatures for different defect cases at 5.625 kW are plotted in Fig. 6a. Similarly, to observe the variation of ECDF with load. Fig. 6b is drawn for d_1 condition. Fig. 6c shows the D -stat variation with load when all the current signatures are compared with current

Table 3 (continued)

	d0:0	d0:1.875	d0:3.75	d0:5.625	d1:0	d1:1.875	d1:3.75	d1:5.625	d2:0	d2:1.875	d2:3.75	d2:5.625	d3:0	d3:1.875	d3:3.75	d3:5.625	d4:0	d4:1.875	d4:3.75	d4:5.625	d5:0	d5:1.875	d5:3.75	d5:5.625		
d4:1.875		H																								
P																										
k																										
d4:3.75		H																								
P																										
k																										
d4:5.625		H																								
P																										
k																										
d5:0		H																								
P																										
k																										
d5:1.875		H																								
P																										
k																										
d5:3.75		H																								
P																										
k																										
d5:5.625		H																								
P																										
k																										

d0:3.75: no defect at 3.75 kW steady load, H: handle to the decision, p: p-value, k: D-stat.

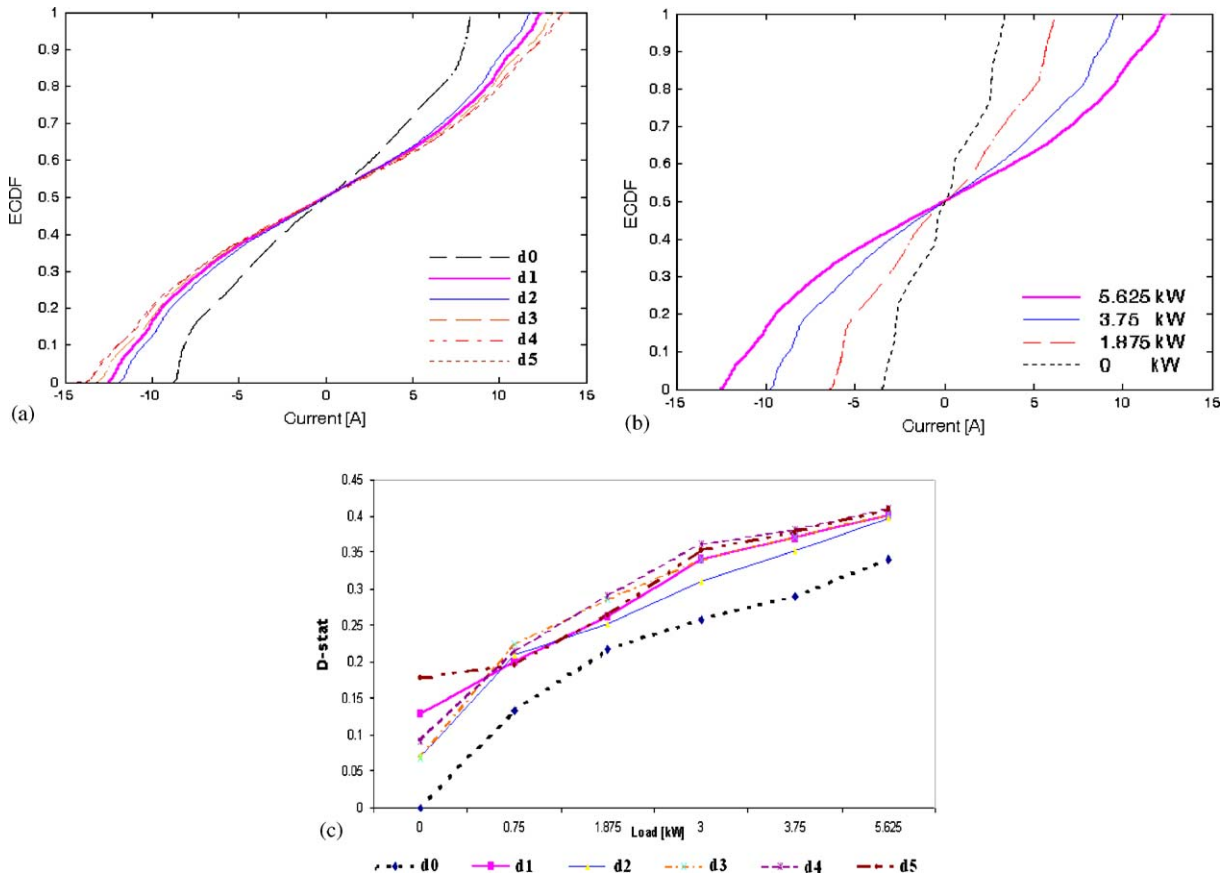


Fig. 6. Summary of Table 3: (a) ECDFs of current signatures of all defective cases at 5.625 kW steady load condition during 2nd gear operation, (b) ECDF of $d1$ at all load conditions, (c) D -stat variation with load when all current signatures are compared with current signature with no load and no defect ($d0:0$).

signature at no load and no defect condition ($d0:0$), in addition to four steady loads, two more steady loads of 0.75 and 3 kW; that are not considered in the table are added in order to confirm the trends. The following inferences are drawn:

1. Unlike vibration signature, when KS test is applied to current signatures, all defects are being able to be separated from no defect case at all steady load conditions. The ECDFs at 5.625 kW steady load condition are distinct and very much different from that of no defective case (Fig. 6a). It is observed that 3rd gear defects ($d4$ and $d5$) draw more current than 2nd gear defective cases during 2nd gear operation.
2. For one tooth broken in 2nd gear ($d1$), the ECDF and hence D -stat is more than those for two teeth broken in 2nd gear ($d2$), inferring that defects can be detected at an early stage.
3. For load variation at a particular case of defect ($d1$ in Fig. 6b), the decrease in ECDFs are more prominent than the same in case of vibration signatures shown in Fig. 4b, and hence can be monitored with more ease.

4. The summary shown in Fig. 6c confirms the above findings that KS test combined with MCSA can be a better technique to detect all types of defects than the same with vibration signatures during 2nd gear operation.

4.1.3. Vibration signatures under steady loads: 3rd gear operation

The time-domain vibration signatures of all defective cases at 5.625 kW steady load condition and during 3rd gear operation revealed that except for d5 defect condition, there is no sign of impact in any other signature, moreover, the vibration level is very low, thus confirming the fact that 3rd gear operation is a much smoother operation than 2nd gear operation. These signatures at all defective and load conditions are tested among themselves, and the summary is shown in Fig. 7. ECDFs for all defective cases at 5.625 kW steady load conditions are plotted in Fig. 7a. Similarly, the ECDFs at all load conditions for a particular defect condition d5 are drawn in

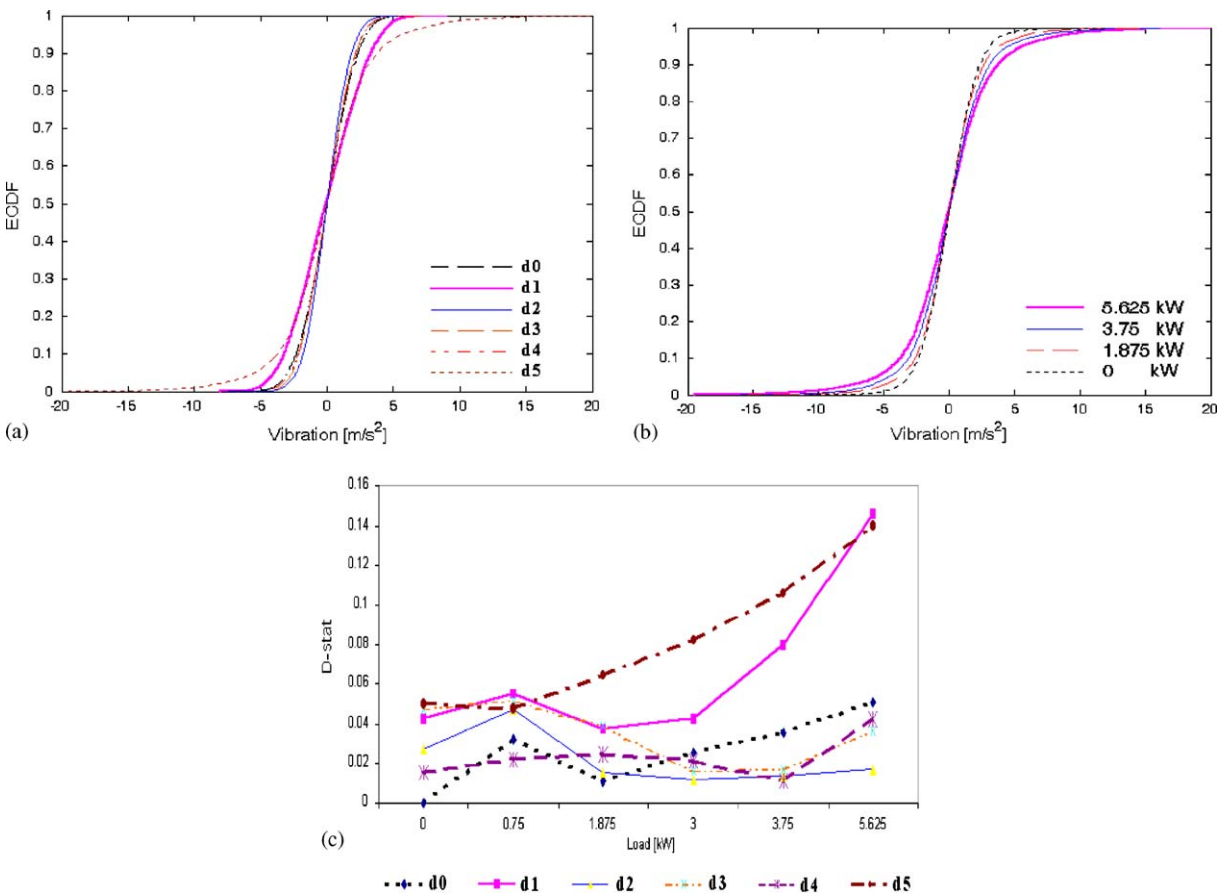


Fig. 7. (a) ECDFs of vibration signatures of all cases of defects at 5.625 kW steady load condition during 3rd gear operation, (b) ECDFs of all load conditions at d5, (c) D-stat variation with load for all defective cases.

Fig. 7b. Fig. 7c indicates the *D*-stat variation with respect to load when compared with vibration signature with no load and no defect condition. The following observations are made:

1. The ECDF of *d5* case is much larger than that of others at 5.625 kW load condition as observed in Fig. 7a. At no load condition (0 kW), all the defects can easily be detected whereas at higher loads, only *d1* and *d5* conditions can be distinguished (Fig. 7c) when compared to signature of no load and no defect conditions.
2. The ECDF decreases with decrease in load below the intersection point as shown in Fig. 7b.

4.1.4. Motor current signatures under steady loads: 3rd gear operation

Current signatures at all steady load conditions and defective cases during 3rd gear operation are compared among themselves, and the summary is illustrated in Fig. 8. The ECDFs at a particular load condition i.e. 5.625 kW are presented in Fig. 8a, the effect of change in load on the

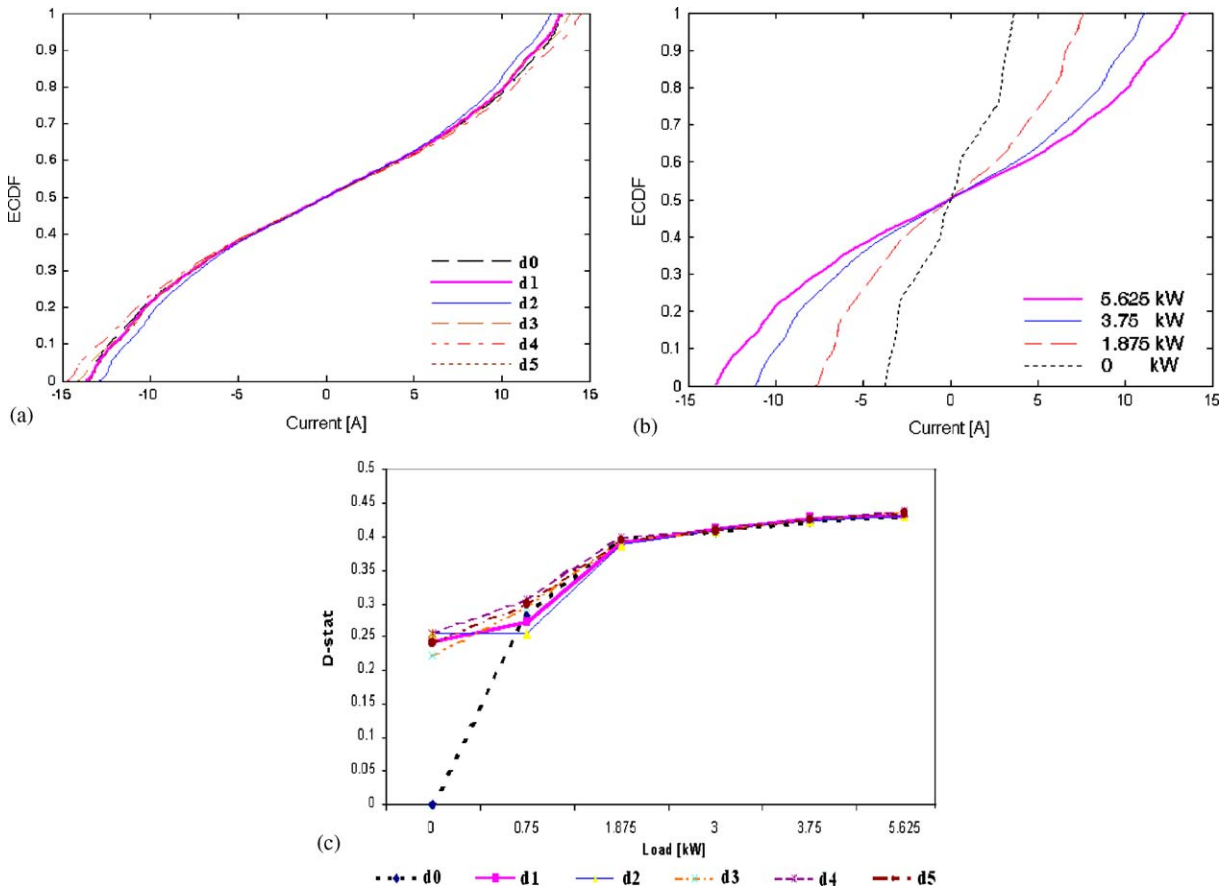


Fig. 8. (a) ECDF of current signatures with all defective gears during 3rd gear operations at 5.625 kW steady load, (b) ECDF of current signatures at all load conditions with *d5* condition, (c) *D*-stat variation with load for all defective gears when current signature at no defect and no load condition is the basis.

ECDF has been described in Fig. 8b, and the D -stat variation with change in load has been shown in Fig. 8c. The following inferences are drawn:

1. All defects can be detected at no load condition, but at higher loads, the D -stat has failed to distinguish faults (Fig. 8c).
2. The ECDFs of current signatures with all defective conditions except $d1$ at 5.625 kW are found to be having distinct ECDF. The ECDF of $d1$ coincides with that of $d0$ and hence could not be distinguished (Fig. 8a). Moreover, the ECDF of $d2$ lies below the ECDF of $d0$ below the intersection point, implying that 2nd gear defects during 3rd gear operation are difficult to be detected.
3. Variation of ECDFs for a particular defect condition i.e. $d5$ with change in load (Fig. 8b) is investigated and found that like earlier cases, there is an appreciable difference in the probability distributions.

4.2. Transients due to load fluctuation

In all the previous sections, it has been found that there is a large variation of ECDF and subsequently variation of D -stat with change in load, and hence there is a possibility that after introducing load fluctuation and capturing the current and vibration transients, faults can be distinguished by applying KS test. The studies of fluctuating load conditions are necessary for the following reasons. First, during starting operation of the gearbox, faults can be detected. Second, in the real operation of gearbox, there is always a large amount of load fluctuation involved. Hence, here three cases of load fluctuations described in Section 3.2 are introduced and the gearbox is operated at 2nd and 3rd gear operations.

4.2.1. Vibration signatures under fluctuating loads: 2nd gear operation

Fig. 9 shows the time-domain vibration transients for all the defective cases at 5.625 kW load fluctuation (Case III). The point of load fluctuation has been centered at 0.2 s in order to avoid any time delay explained in Appendix A. The variation in amplitude of vibration and the sign of impact can clearly be seen. The result of D -stat and p -values when KS test is applied to vibration transients are shown in Table 4. The following observations are found:

1. At $d0$ and $d5$ cases, the load fluctuation does not change the amplitude distribution.
2. Vibration signature with $d0$:I is found to be having same probability distribution as vibration signatures with $d1$:II and $d3$:I conditions. The ECDFs for vibration signatures with all the defective cases at 5.625 kW load fluctuation are shown in Fig. 10a, and it is found that ECDF variation with defects are inconsistent, even the ECDFs of signatures with 3rd gear defects are much lesser than the no defect and 1.875 kW fluctuating load condition.
3. But for a particular defective condition ($d1$), the ECDF is found to be decreasing with decrease in fluctuating loads below the intersection point (shown in Fig. 10b), which has been observed in other defective conditions.
4. When compared with the vibration signatures at 1.875 kW load fluctuation and no defect, the D -stat for 3rd gear defects are found to be appreciably larger than those of 2nd gear defects during 2nd gear operation (Fig. 10c), a trend that is in contradiction with that during steady

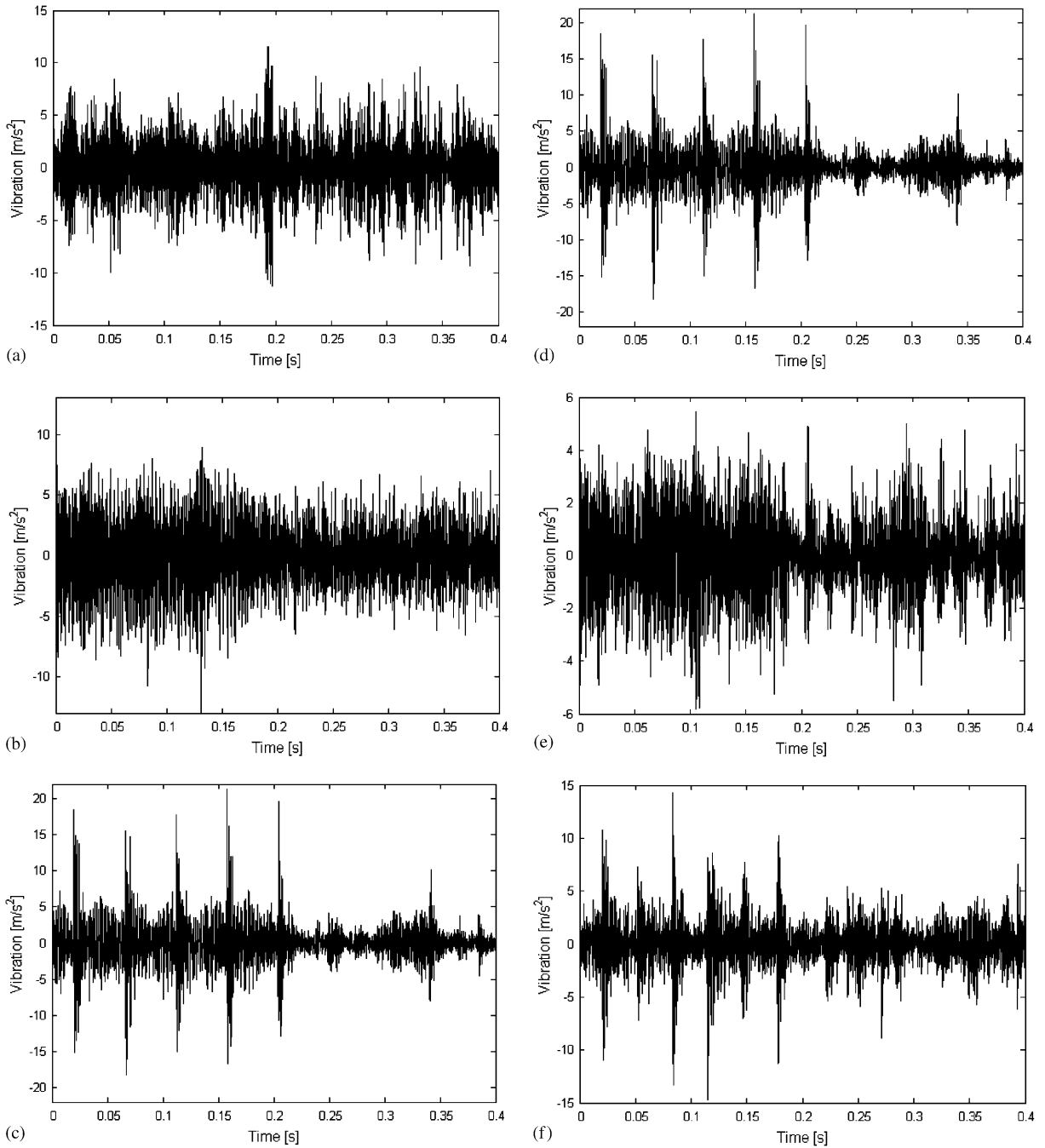


Fig. 9. The time-domain vibration transients for all defective cases with 5.625 kW load fluctuation: (a) *d0*, (b) *d1*, (c) *d2*, (d) *d3*, (e) *d4*, and (f) *d5*.

Table 4
KS test parameters for vibration transients during 2nd gear operation

		d0:I	d0:II	d0:III	d1:I	d1:II	d1:III	d2:I	d2:II	d2:III	d3:I	d3:II	d3:III	d4:I	d4:II	d4:III	d5:I	d5:II	d5: III
d0:I	H	0	0	0	1	0	1	1	1	1	0	1	1	1	1	1	1	1	1
	p	1	0.0683	0.4967	0.0002	0.3508	0	0	0.0002	0.0001	0.3408	0	0.0073	0	0	0	0	0	0
	k	0	0.0203	0.0129	0.0332	0.0145	0.0571	0.0463	0.0333	0.0341	0.0146	0.051	0.0261	0.1115	0.1321	0.115	0.0873	0.0968	0.0762
d0:II	H	0	0	0	1	1	1	1	1	1	1	1	1	1	1	1	1	1	1
	p	1	0.0868	0	0.0032	0	0	0	0	0.0008	0.0001	0.0164	0	0	0	0	0	0	0
	k	0	0.0195	0.0491	0.028	0.0488	0.0614	0.0505	0.0507	0.0306	0.0337	0.0242	0.129	0.1503	0.1311	0.1039	0.1125	0.0907	
d0:III	H	0	0	1	0	1	1	1	1	0	1	1	1	1	1	1	1	1	1
	p	1	0	0	0.2438	0	0	0	0	0.5468	0	0.0095	0	0	0	0	0	0	0
	k	0	0.0359	0.016	0.056	0.0547	0.415	0.043	0.0125	0.0457	0.0255	0.1148	0.1377	0.1182	0.0907	0.0966	0.0764		
d1:I	H	0	0	1	1	0	0	0	0	1	1	1	0	1	1	1	1	1	1
	p	1	0.0006	0	0.0533	0.2517	0.1053	0.0001	0	0	0	0	0	0	0	0	0	0	0
	k	0	0.0311	0.0836	0.021	0.0159	0.0189	0.0342	0.0769	0.0409	0.0903	0.1099	0.0872	0.0677	0.0742	0.0511			
d1:II	H	0	1	1	1	1	1	0	1	0	1	0	1	1	1	1	1	1	1
	p	1	0	0	0	0	0	0	0.0683	0	0.0604	0	0	0	0	0	0	0	0
	k	0	0.586	0.0425	0.0371	0.0355	0.0203	0.0531	0.0206	0.1143	0.1327	0.1122	0.0953	0.0981	0.0769				
d1:III	H	0	0	1	1	1	1	1	1	1	1	1	1	1	1	1	1	1	1
	p	1	0	0	0	0	0	0	0.0004	0	0	0	0	0	0	0	0	0	0
	k	0	0.0956	0.0864	0.083	0.0664	0.0319	0.0504	0.1665	0.1866	0.1666	0.1403	0.1486	0.129					
d2:I	H	0	0	1	1	1	1	1	1	1	1	1	1	1	1	1	1	1	1
	p	1	0	0	0	0	0	0	0	0	0	0	0	0	0	0	0	0	0
	k	0	0.0231	0.0262	0.0509	0.0923	0.0526	0.0792	0.0963	0.0797	0.059	0.063	0.0442						
d2:II	H	0	1	1	0	1	1	1	1	1	1	1	1	1	1	1	1	0	1
	p	1	0	0	0	0	0	0	0	0	0	0	0	0	0	0	0	1	0
	k	0	0.0229	0.036	0.0798	0.0447	0.0842	0.1095	0.0925	0.0667	0.0743	0.0554							
d2:III	H	0	1	1	1	1	1	1	1	1	1	1	1	1	1	1	1	1	1
	p	1	0	0	0	0	0	0	0	0	0	0	0	0	0	0	0	0	0
	k	0	0.0402	0.0745	0.0477	0.0977	0.1133	0.0964	0.0773	0.0826	0.0593								
d3:I	H	0	1	1	1	1	1	1	1	1	1	1	1	1	1	1	1	1	1
	p	1	0	0.0031	0	0	0	0	0	0	0	0	0	0	0	0	0	0	0
	k	0	0.0476	0.0281	0.1144	0.1382	0.115	0.0897	0.094	0.0732									
d3:II	H	0	1	1	1	1	1	1	1	1	1	1	1	1	1	1	1	1	1
	p	1	0	0	0	0	0	0	0	0	0	0	0	0	0	0	0	0	0
	k	0	0.0405	0.1577	0.1814	0.1588	0.1346	0.1392	0.1174										
d3:III	H	0	1	1	1	1	1	1	1	1	1	1	1	1	1	1	1	1	1
	p	1	0	0	0	0	0	0	0	0	0	0	0	0	0	0	0	0	0
	k	0	0.1252	0.1455	0.1227	0.1034	0.1089	0.085											
d4:I	H	0	1	1	1	1	1	1	1	1	1	1	1	1	1	1	1	1	1
	P	1	0.0003	0.0345	0.0022	0.0164	0												
	k	0	0.0326	0.0222	0.0288	0.0242	0.0437												
d4:II	H	0	1	1	1	1	1	1	1	1	1	1	1	1	1	1	1	1	1
	P	1	0.0105	0	0	0	0	0	0	0	0	0	0	0	0	0	0	0	0
	k	0	0.0253	0.0558	0.0508	0.0668													
d4:III	H	0	1	1	1	1	1	1	1	1	1	1	1	1	1	1	1	1	1
	P	1	0	0	0	0	0	0	0	0	0	0	0	0	0	0	0	0	0
	k	0	0.0415	0.0359	0.0535														
d5:I	H	0	0	0	0	0	0	0	0	0	0	0	0	0	0	0	0	0	0
	P	1	0	0.5596	0.0835														
	K	0	0.0123	0.0197															
d5:II	H	0	1	1	1	1	1	1	1	1	1	1	1	1	1	1	1	1	1
	P	1	0.0066																
	k	0	0.0264																
d5:III	H	0	0	0	0	0	0	0	0	0	0	0	0	0	0	0	0	0	0
	P	1	0	0	0	0	0	0	0	0	0	0	0	0	0	0	0	0	0
	k	0	0	0	0	0	0	0	0	0	0	0	0	0	0	0	0	0	0

I Case-I: load fluctuation from 1.875 to 0kW, II Case-II load fluctuation from 3.75 to 0kW, III Case-III load fluctuation from 5.625 to 0kW.

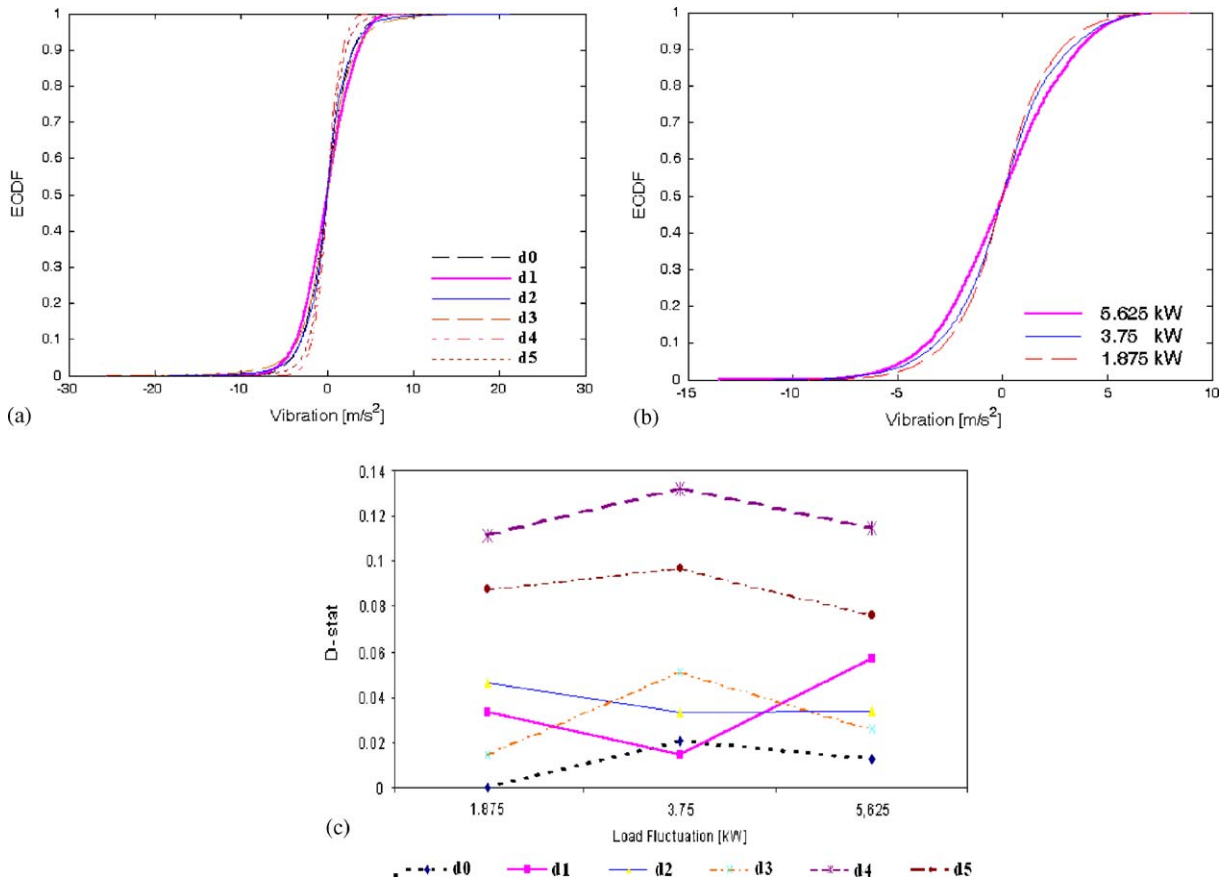


Fig. 10. Summary of Table 4: (a) ECDF of vibration transients with all defective cases during 2nd gear operation at 5.625 kW fluctuating load condition, (b) ECDF of vibration transients for defective *d1* cases at all load fluctuation, (c) *D*-stat variation with load fluctuation when all transients are compared with transient with no load and no defect.

load operation. The reason is that load fluctuation affects the 3rd gear the most since load acts as a damping factor, and removal of load changes the vibration level. It is also difficult to diagnose *d1* at 3.75 kW load fluctuation (Fig. 10).

4.2.2. Current transients under fluctuating loads: 2nd gear operation

The time-domain current signature for no defect and 5.625 kW fluctuating load is shown in Fig. 11. For all other cases, the figures have only difference in their amplitudes and rate of decays, and hence not been shown. The fluctuation has been kept at the center of the time so that there is not much time-lagging for all the cases. The effect of time-lagging has been discussed in Appendix A. Table 5 shows the *D*-stats and corresponding *p*-values for current transients with all defects and load fluctuations when compared among them. The following observations are noted:

1. As inferred during steady current signature at 2nd gear operation, the same observation is noted that all defects can be diagnosed when the ECDFs are observed for a particular

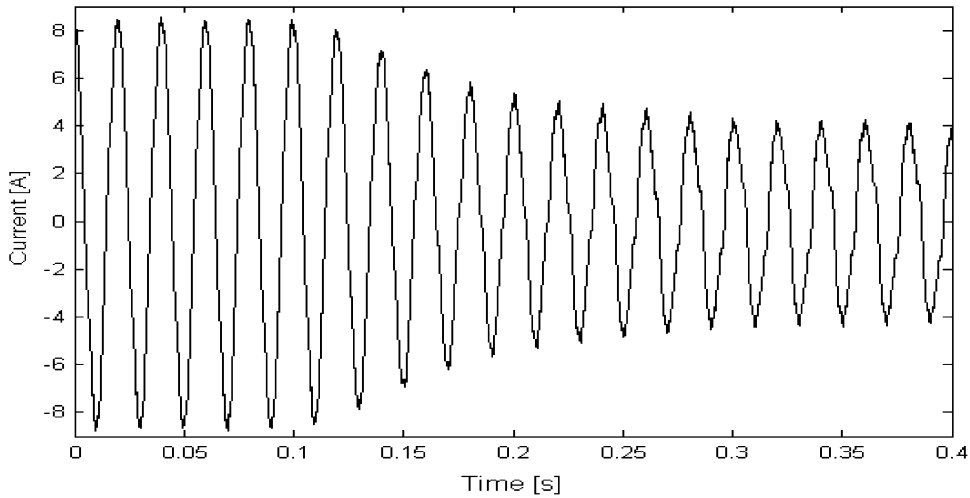


Fig. 11. Time-domain current transient due to 5.625 kW load fluctuation for no defect condition.

fluctuating load conditions (5.625 kW load shown in Fig. 12a). Even, 3rd gear defects draw more current and have higher ECDFs than 2nd gear defects. But when the D -stat variation with load fluctuation is observed, $d5$, $d1$ and $d3$ have larger D -stat values than other cases as shown in Fig. 12c.

2. One tooth defects in both 2nd gear ($d1$) and 3rd gear ($d4$) have same probability distribution of amplitudes of current at 5.625 kW load conditions.
3. Load fluctuation is more prominent in current transients than vibration transients at a particular defect conditions, $d1$ shown in Fig. 12b.

4.2.3. Vibration signatures under fluctuating loads: 3rd gear operation

The vibration transients due to fluctuating loads for all defective load conditions are tested and results are summarized in Fig. 13. The following conclusions are drawn:

1. Referring to Fig. 13a, it has been found that ECDFs are inconsistent except for $d5$ case which causes severe vibration in the gearbox conformed while studying the steady vibration signatures. Similarly, load fluctuation is also causing inconsistent ECDF except at 5.625 kW when defect $d5$ case is considered, shown in Fig. 13b.
2. Defects in all gears (except lay shaft gear at 5.625 kW) can be distinguished as shown in Fig. 13c. But two defects in 3rd gear will cause severe vibration than the other cases.

4.2.4. Current signatures under fluctuating loads: 3rd gear operation

Fig. 14 summarizes the results of KS test for current transients with several defects and load fluctuations. The following observations are made:

1. Fig. 14a indicates that among all the ECDFs of defective cases of current transients at 5.625 kW load fluctuation, $d4$ not only draws more current, but also is having higher ECDF,

Table 5
KS test parameters for current transients during 2nd gear operation

		d0:I	d0:II	d0:III	d1:I	d1:II	d1:III	d2:I	d2:II	d2:III	d3:I	d3:II	d3:III	d4:I	d4:II	d4:III	d5:I	d5:II	d5: III
d0:I	H	0	1	1	1	1	1	1	1	1	1	1	1	1	1	1	1	1	1
	p	1	0	0	0	0	0	0	0	0	0	0	0	0	0	0	0	0	0
	k	0	0.078	0.1083	0.0608	0.1359	0.1503	0.0541	0.1055	0.1447	0.0823	0.1158	0.1887	0.0612	0.11	0.1337	0.0502	0.1412	0.1565
d0:II	H		0	1	1	1	1	1	1	1	1	1	1	1	1	1	1	1	1
	p		1	0	0	0	0	0	0	0	0	0	0	0	0	0	0	0	0
	k		0	0.062	0.0532	0.0824	0.1058	0.0669	0.0537	0.1027	0.0389	0.0747	0.1361	0.0352	0.0677	0.0906	0.0614	0.0863	0.1113
d0:III	H			0	1	1	1	1	1	1	1	1	1	1	1	1	1	1	1
	p			1	0	0	0	0	0.0056	0	0.004	0	0	0.0005	0	0	0	0	0
	k			0	0.0839	0.0383	0.0762	0.0981	0.0267	0.0682	0.0729	0.0275	0.1021	0.0718	0.0317	0.064	0.1097	0.0385	0.08
d1:I	H				0	1	1	1	1	1	1	1	1	0	1	1	1	1	1
	p				1	0	0	0.0005	0	0	0	0	0	0.0156	0	0	0	0	0
	k				0	0.1086	0.1246	0.0317	0.0781	0.1256	0.0616	0.0958	0.1571	0.0243	0.0874	0.1078	0.0481	0.1133	0.1318
d1:II	H					0	1	1	1	1	1	1	1	0	1	1	1	1	1
	p					1	0	0	0	0	0	0.024	0	0	1	0	0	0	0
	k					0	0.0503	0.1201	0.0455	0.0386	0.0919	0.0232	0.0687	0.0914	0.0488	0.0432	0.1223	0.035	0.0562
d1:III	H						U	1	1	U	1	1	1	1	1	0	1	1	0
	p						1	0	0	0.058	0	0	0	0	0.0511	0	0	0.2361	
	k						0	0.1389	0.073	0.0208	0.1111	0.0527	0.0557	0.1134	0.0577	0.0211	0.1257	0.0553	0.0161
d2:I	H							0	1	1	1	1	1	1	1	1	1	1	1
	p							1	0	0	0	0	0	0	0	0	0	0	0
	k							0	0.0933	0.1344	0.0642	0.1036	0.1741	0.0369	0.0996	0.1212	0.0441	0.1288	0.1449
d2:II	H								0	1	1	1	1	1	1	1	1	1	1
	p								1	0	0	0	0	0	0	0	0	0	0
	k								0	0.0699	0.0679	0.042	0.098	0.0667	0.0377	0.0605	0.089	0.0436	0.0769
d2:III	H								0	1	1	1	1	1	1	1	1	1	1
	p								1	0	0	0	0	0	0.0021	0	0	0.0007	
	k								0	0.1118	0.0483	0.0502	0.1108	0.0502	0.0289	0.1246	0.0417	0.031	
d3:I	H									0	1	1	1	1	1	1	1	1	1
	p									1	0	0	0	0	0	0	0	0	0
	k									0	0.0798	0.1409	0.0511	0.0771	0.0973	0.0884	0.1006	0.1169	
d3:II	H										0	1	1	1	1	1	1	1	1
	p										1	0	0	0	0	0	0.0001	0	
	k										0	0.0764	0.0823	0.0483	0.0454	0.1243	0.0341	0.0581	
d3:III	H											0	1	1	1	1	1	1	1
	p											1	0	0	0	0	0	0	0
	k											0	0.1449	0.0958	0.0657	0.161	0.0745	0.0536	
d4:I	H													0	1	1	1	1	1
	p													1	0	0	0	0	0
	k													0	0.0757	0.0959	0.058	0.0995	0.1176
d4:II	H														0	1	1	1	1
	p														1	0	0	0	0
	k														0	0.0428	0.1148	0.051	0.0619
d4:III	H															0	1	1	1
	p															1	0	0	0.0048
	k															0	0.109	0.0454	0.0271
d5:I	H																0	1	1
	p																1	0	0
	k																0	0.1138	0.1323
d5:II	H																	0	1
	p																	1	0
	k																	0	0.0594
d5:III	H																		0
	p																		1
	k																		0

I Case-I: load fluctuation from 1.875 to 0kW, II Case-II load fluctuation from 3.75 to 0kW, III Case-III load fluctuation from 5.625 to 0kW.

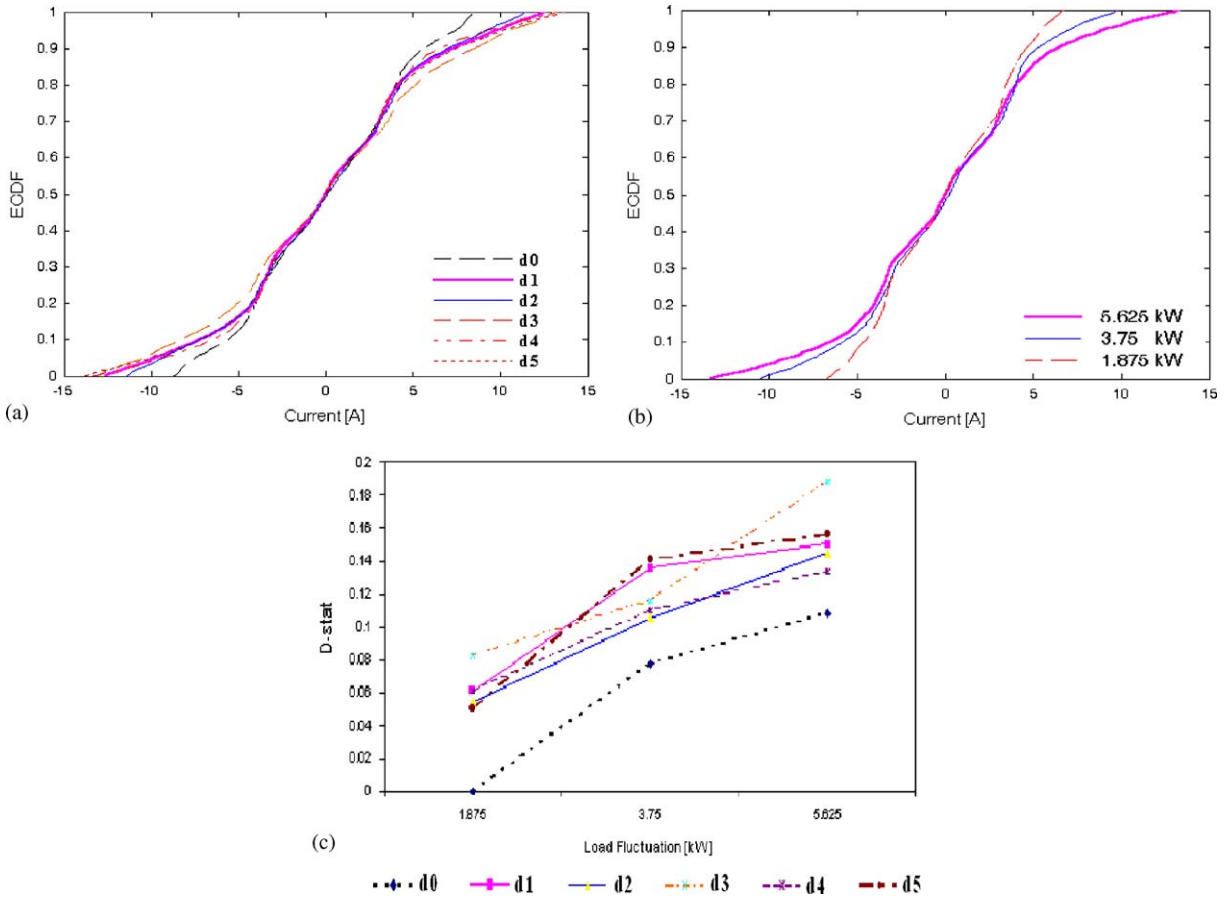


Fig. 12. Summary of Table 5: (a) ECDF of current transients with all defective cases during 2nd gear operation at 5.625 kW load fluctuation, (b) ECDF of current transients with all fluctuating load conditions for *d1* case, (c) *D*-stat variation with change in fluctuating load when compared to current transients at no defect and no load.

the same inference has been drawn for current under steady load during 3rd gear operation (Fig. 14a). But, this is in contradiction to the corresponding vibration signatures (Figs. 7a and 13a) where *d5* condition is having most severe vibration levels. This makes the study of current signatures more attractive as the early indication of defect in 3rd gear (one defect) can be easily detected during 3rd gear operation.

2. Amount of load fluctuation affects the ECDFs in the same way as described in earlier cases but with a prominent difference than that of vibration signatures. Fig. 14b shows the effect of load fluctuation on ECDFs of current transients for *d4* case.
3. Fig. 14c indicates that except 2 defects in 2nd gear with high load fluctuation, all other defects can be separated from no defect gears while studying current transients during 3rd gear operation.

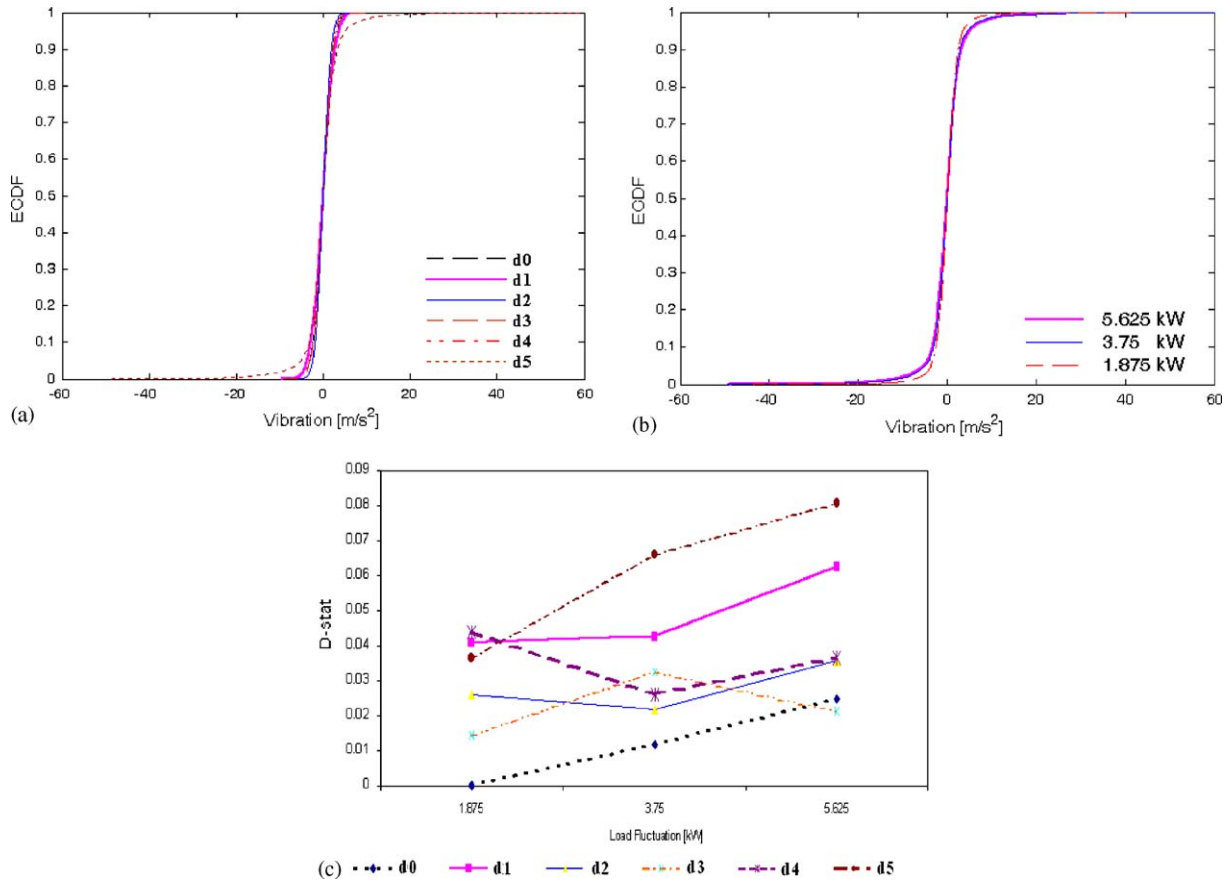


Fig. 13. (a) ECDFs of vibration transients of all defective gears during 3rd gear operation at 5.625 kW load fluctuation, (b) ECDFs for *d5* defect conditions with all load fluctuation conditions, (c) *D*-stat variation with load of all cases of defects considering vibration transient with no defect and 1.875 kW load fluctuation as basis.

5. Conclusion

This paper considered both vibration and current signatures during steady and fluctuating load conditions of 2nd and 3rd gear operation of a multistage automotive transmission gearbox. The objective was to diagnose different types of faults in gears using combined MCSA and KS test. The following inferences are observed:

1. MCSA combined with KS test can be a better technique than monitoring vibration signatures using KS test for the following reasons:
 - a. Defects in 2nd and 3rd gear can easily be detected at all steady load conditions during both 2nd and 3rd gear operations by monitoring current signature only. Whereas while studying vibration signatures under steady loads, only defects of 2nd gear during 2nd gear operation; and one defect in 2nd gear and two defects in 3rd gear during 3rd gear operation could be

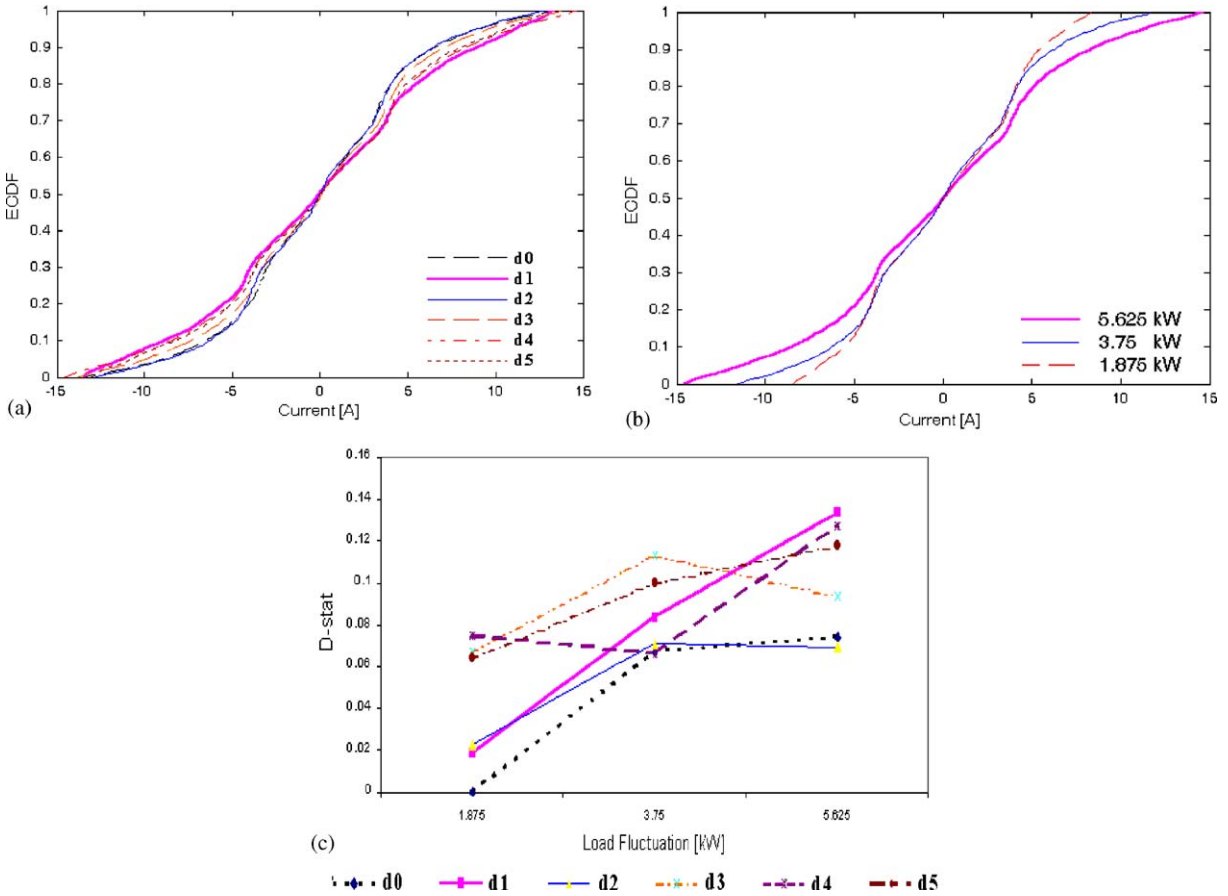


Fig. 14. (a) ECDFs of current transients for all defective cases during 3rd gear operation at 5.625 kW load fluctuation, (b) ECDFs of current transients for *d4* case for all load fluctuation conditions, (c) *D*-stat variation with load fluctuation for all defective current transients when compared with the current transient with no defect and 1.875 kW load fluctuation.

diagnosed. For transients both in vibration and current due to fluctuating load, the same observations are noted except for 2 defects in 2nd gear during 3rd gear operation in the current transient.

- b. Study of ECDF suggest that early indication of gear defects can be found using current signature analysis for both steady and transient operation during both 2nd and 3rd gear operations. Whereas for vibration signatures, only for 2nd gear steady operation, the same inference can be drawn.
 - c. With load fluctuation for a particular defect case, the decrease of ECDFs is more prominent in current than those in vibration signatures.
2. The time-domain signatures and DWT contour diagrams suggest that vibration signatures with two defects in 2nd gear and 2nd gear layshaft gear during 2nd gear operation have higher

maximum amplitude of vibration, but lower ECDF than those in 1 defect in 2nd gear. The 3rd gear defects are difficult to be traced during 2nd gear operation.

Hence, it is concluded that when there is a large variation in torque as during the 2nd gear operation in our study, any type of defects can be easily monitored using MCSA and KS test. Small defects in a helical gear such as one tooth broken could be monitored even at no load and 0.75 kW load in this paper. These findings can lead to develop an expert system, which can be helpful for online fault diagnosis in the gearbox. In this work, it has been well established that in a multistage automotive transmission gearbox; which poses complex vibration behavior with the presence of lay-shaft, and varying transmission path in the gearbox during different operations; the faults can be easily diagnosed with MCSA and KS test. Thus, this has a very wide range of application in industries where many types of gearboxes are found.

Appendix A

This appendix contains examples of calculation of D -stat from the ECDF and effects of some important parameters such as DC component, noise and time-lagging on D -stat.

A.1. Critical value of D -stat

Since 8192 number of data points are used for all cases of steady and transient signatures, the critical value of D -stat (D_{critical}) will be constant for the KS test in this paper. Using Eq. (17), the D_{critical} is found to be 0.0212 for 5% significance level. If $D\text{-stat} > D_{\text{critical}}$, then p -value will be less than 0.05 for which $H = 1$ (that is the alternate hypothesis is accepted in favor of null hypothesis: two data sets have different probability distribution). For two vibration signatures shown in Figs. 3a and c, the ECDFs are plotted in Fig. A.1. The D -stat is the maximum difference between the two ECDFs mentioned in Eq. (9).

A.2. Effect of DC component

Before applying KS test, care must be taken to remove the DC component, otherwise the D -stat will give erroneous result. Fig. A.2 shows an example where the signal shown in Fig. 3c is compared with itself before removal of its DC component (-0.261), and the result of D -stat is 0.0461 giving a p -value of 0, and hence $H = 1$, thus giving an erroneous result that the two data sets are not equal.

A.3. Effect of signal to noise ratio (SNR)

While using the anti-aliasing low pass filter during data acquisition, appropriate gain must be applied to improve the signal to noise ratio as the poor SNR gives erroneous result. Fig. 13 shows the current transient acquired with appropriate gain and when it compared with a noisy current signal, then the ECDFs are distinct and D -stat is found to be as high as 0.1082 (as illustrated in Fig. A.3).

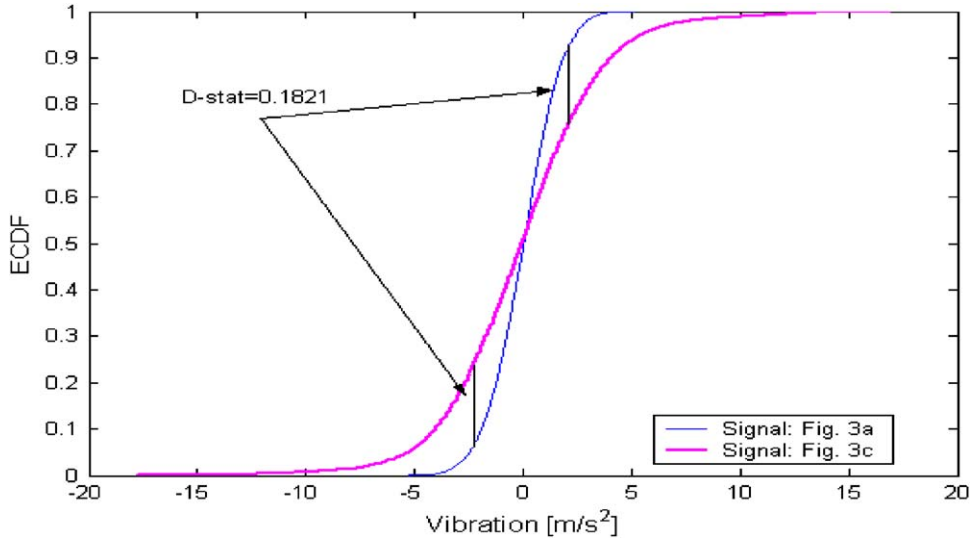


Fig. A.1. *D*-stat for two vibration signatures shown in Figs. 3(a) and (c).

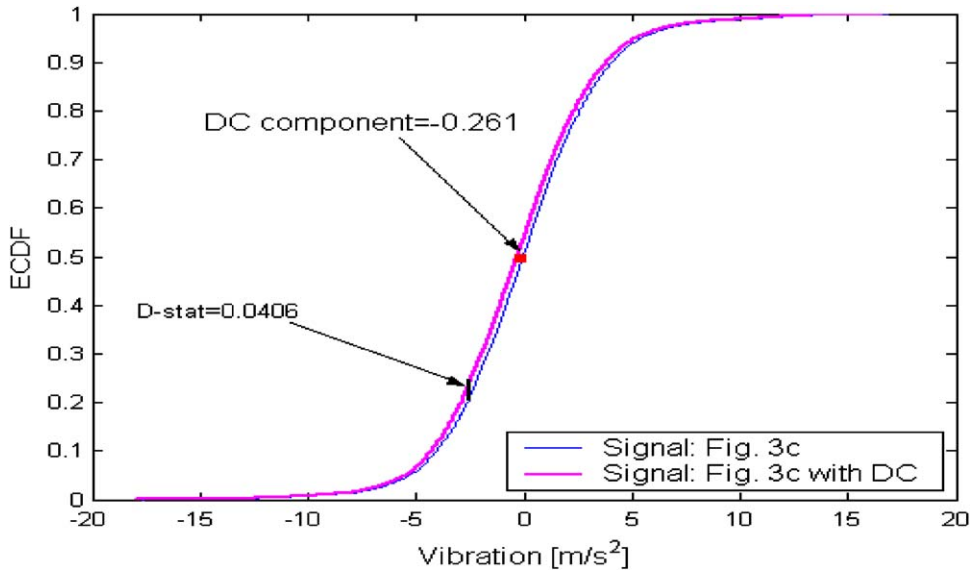


Fig. A.2. The effect of DC component for vibration signal of Fig. 3c.

A.4. Effect of time-lagging

The effect of time-lagging during steady load operation has already been discussed in Ref. [12] that when the time record takes into account a number of revolutions of the shaft, then the time-lagging does not affect the *D*-stat value. Hence, for the steady signatures of vibration and current,

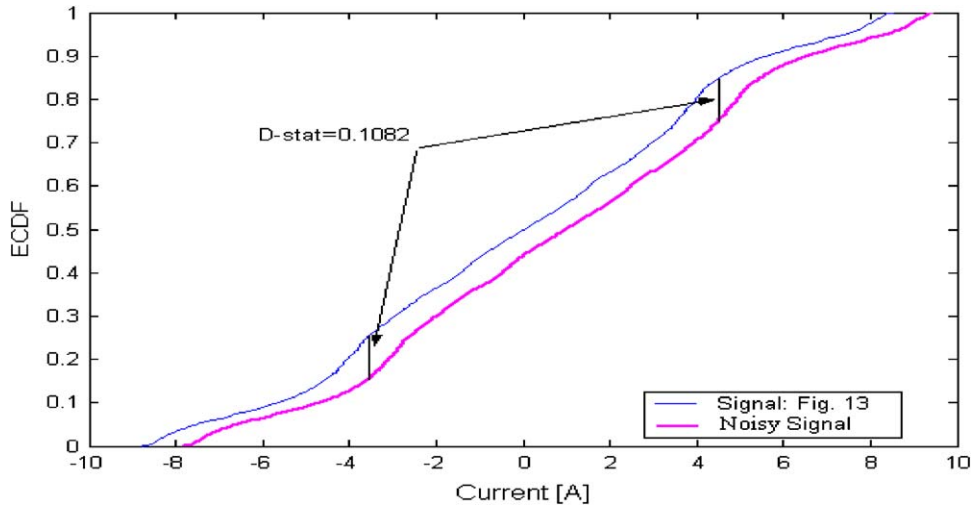


Fig. A.3. ECDFs of the noisy and noise free signal of Fig. 13.

the time-lagging does not play any role in this paper as 2 s record time will accommodate around 100 revolutions of input shaft (considering about 49 Hz input shaft speed). But, for the case of study of transients due to load fluctuation, the time lagging will hamper the result and hence, care has been taken to accommodate the load fluctuation at the center of the time record.

References

- [1] M.E.H. Benbouzid, A review of induction motor signature analysis as a medium for faults detection, *IEEE Transactions on Industrial Electronics* 47 (5) (2000) 984–993.
- [2] S. Nandi, H.A. Toliyat, Condition monitoring and fault diagnosis of electrical machines—a review, *IEEE 34th IAS annual meeting, Industry Application Conference* 1 (1999) 197–204.
- [3] C. Kar, A.R. Mohanty, Monitoring gear vibrations through motor current signature analysis and wavelet transform, *Mechanical Systems and Signal Processing* (2004) in press, doi:10.1016/j.ymssp.2004.07.006.
- [4] A.R. Mohanty, C. Kar, Gearbox health monitoring through three phase motor current signature analysis, in: *Proceedings of Fourth International Workshop on Structural Health Monitoring*, Stanford University, USA, 2003, pp. 1366–1373.
- [5] R.B. Randal, J. Hee, Cepstrum analysis, *Bruel and Kjaer Technical Review* (3) (1981).
- [6] N. Bayder, A. Ball, A comparative study of acoustic and vibration signals in detection of gear failures using Weigner–Ville distribution, *Mechanical Systems and Signal Processing* 15 (6) (2001) 1091–1107.
- [7] W.J. Wang, P.D. McFadden, Application of wavelets to gearbox vibration signals for fault detection, *Journal of Sound and Vibration* 192 (5) (1996) 927–939.
- [8] D.C.D. Oguamanam, H.R. Martin, J.P. Huissoon, On the application of the beta distribution to gear damage analysis, *Applied Acoustics* 45 (1995) 247–261.
- [9] J.D. Jiang, J. Chen, L.S. Qu, The application of correlation dimension in gearbox condition monitoring, *Journal of Sound and Vibration* 223 (4) (1999) 529–541.
- [10] F.A. Andrede, I. Isat, M.N.M. Badi, A new approach to time-domain vibration condition monitoring: gear tooth fatigue crack detection and identification by the Kolmogorov–Smirnov test, *Journal of Sound and Vibration* 240 (5) (2001) 909–919.

- [11] F.A. Andrede, I. Isat, M.N.M. Badi, Gear condition monitoring by a new application of the Kolmogorov–Smirnov test, *Proceeding of the Institute of Mechanical Engineers–Part C* 215 (2002) 793–800.
- [12] C. Kar, A.R. Mohanty, Application of K S test in ball bearing fault diagnosis, *Journal of Sound & Vibration* 269 (1–2) (2004) 439–454.
- [13] L.D. Hall, D. Mba, Acoustic emissions diagnosis of rotor-stator rubs using the KS statistic, *Mechanical Systems and Signal Processing* 18 (2004) 849–868.
- [14] W.J. Staszewski, G.R. Tomilson, Application of wavelet transform to fault detection in spur gear, *Mechanical Systems and Signal Processing* 8 (3) (1994) 289–307.
- [15] C. Kar, A.R. Mohanty, Time-varying parameters in vibration excitation of helical gears, in: *Proceedings of Third International Conference on Theoretical, Applied, Computational and Experimental Mechanics*, IIT, Kharagpur, 2004, pp. 1–14.
- [16] F.K. Choy, D.H. Mugler, Damage identification of a gear transmission using vibration signatures, *ASME Journal of Mechanical Design* 125 (2003) 394–403.
- [17] L. Ran, R. Yacamini, K.S. Smith, Torsional vibrations in electrical induction motor drives during start-up, *Journal of Vibration and Acoustics, Transaction of ASME* 118 (1996) 241–251.
- [18] L. Eren, M.J. Devany, Motor bearing damage detection via wavelet analysis of the starting current transients, *IEEE Instruments and Measurement Technology Conference* (2001) 1797–1800.
- [19] R.R. Schoen, T.G. Habetler, Effects of time-varying loads on rotor fault detection in induction machines, *IEEE Transaction on Industry Application* 31 (4) (1995) 900–906.
- [20] R. Yacamini, K.S. Smith, L. Ran, Monitoring torsional vibrations of electro-mechanical systems using stator currents, *Journal of Vibration and Acoustics, Transaction of ASME* 120 (1998) 72–79.
- [21] M.H. Zhang, Q.S. Cheng, Determine the number of components in a mixture model by the extended KS test, *Pattern Recognition Letter* 25 (2004) 211–216.
- [22] S. Ferryanto, A Kolmogorov–Smirnov type statistic for detecting structural changes of textures, *Pattern Recognition Letter* 16 (1995) 247–256.
- [23] W.J. Conover, *Practical Non-parametric Statistics*, Wiley, New York, 1999 pp. 428–465.
- [24] R.N. Greenwell, S.J. Finch, Randomized rejection procedure for the two-sample Kolmogorov–Smirnov statistic, *Computational Statistics & Data Analysis* 46 (2) (2004) 257–267.
- [25] G. Kozmann, L.S. Green, R.L. Lux, Nonparametric identification of discriminative information in body surface maps, *IEEE Transactions on Bio-medical Engineering* 38 (11) (1991) 1061–1068.
- [26] A.M. Albano, P.E. Rapp, Kolmogorov–Smirnov test distinguishes attractors of similar dimension, *Physical Review E* 52 (1) (1995) 196–206.
- [27] D. Zwillinger, S. Kokoska, *CRC Standard Probability and Statistics Tables and Formulae*, Chapman & Hall/CRC, London, 2000 pp. 346–350.